Deformable Patterned Fabric Defect Detection With Fisher Criterion-Based Deep Learning

Yundong Li, Weigang Zhao, and Jiahao Pan

***Abstract*—In this paper, we propose a discriminative representation for patterned fabric defect detection when only limited negative samples are available. Fabric patches are efficiently classified into defectless and defective categories by Fisher criterion-based stacked denoising autoencoders (FCSDA). First, fabric images are divided into patches of the same size, and both defective and defectless samples are utilized to train FCSDA. Second, test patches are classified through FCSDA into defective and defectless categories. Finally, the residual between the reconstructed image and defective patch is calculated, and the defect is located by thresholding. Experimental results demonstrate the effectiveness of the proposed scheme in the defect detection for periodic patterned fabric and more complex jacquard warp-knitted fabric.**

***Note to Practitioners*—Fabric defect detection is an important measure for quality control in a textile factory. The author has conducted a research on defect detection for plain warp-knitted fabric and developed an automatic defect inspection system for textile factories. Based on this previous research, this paper focuses on defect detection for more complex fabric. Deep learning is introduced into this field for the first time. The proposed method provides a new idea for practitioners working on defect detection. In the future, we would like to explore how to integrate this method into an automatic defect inspection system.**

***Index Terms*—Deep learning, denoising autoencoder (DA), fabric defect detection, Fisher criterion, patterned fabric.**

I. Introduction

DEFECT detection is highly important for fabric quality control. Traditionally, defects are detected by human eyes. The efficiency of this manual method is low and the missed rate is high because of eye fatigue. Hence, an automatic inspection system is necessary for textile industries. In the literature, fabric defect detection methods were categorized into six groups: statistical, spectral, model-based, learning, structural, and motif-based [1], [2]. Spectral and structural methods, as well as defects classification by neural networks, are still popular topics in this field. Spectral methods include Fourier transform, wavelet transform, Gabor transform, and so on. Fourier transform is the classic method for fabric analysis. However, Fourier transform was usually used with other approaches in the latest works [2]–[5]. Schneider presented an automatic method for plain and twill fabric detection by combining Fourier analysis, template matching and fuzzy clustering [2]. The system proved to be robust and versatile as a 97% detection accuracy could be achieved. An unsupervised approach for the inspection of periodic pattern fabric by applying Fourier analysis and wavelet shrinkage was proposed [3]. The advantage of this method is that no reference image is needed. Wavelet transform elicited much attention in the fabric detection field because of its good local time-frequency characteristics [6]–[9]. This approach performs well in defects with outstanding edges but poorly in flat defects with smooth grayscale differences. Gabor filters are suitable for emulating the biological features of human eyes and were employed in fabric detection [10]–[13]. However, given that Gabor filters perform filtering at multiscale and multidirection, which result in high-computational complexity, real-time requirements are difficult to meet. To decrease the computational complexity, optimal Gabor filters are built via the genetic algorithm, in which the filters are only performed at one scale and one direction [11], [13]. In recent years, neural networks have also been utilized for fabric defect detection and classification [14], [15]. In addition to the classic backpropagation (BP) networks, an emerging neural networks, namely, pulse-coupled neural networks (PCNN), is also applied to identify defects on plain fabric [16], [17].

Defect inspection has been intensively focused on the plain and twill fabric. Compared with detecting plain and twill defects, patterned fabric defect detection is far more complex. Ng *et al.* gave detail literature of patterned fabric defect detection [18]. To deal with patterned fabric defects, Ng *et al.* presented a novel method by decomposing the target image into cartoon structure as defective objects and texture structure as repeated patterns according to the image decomposition method (ID) [18], [19]. Experimental results showed that the ID method could obtain the state-of-the-art results on periodic patterned fabric [18]. Jing *et al.* filtered a patterned image with optimal Gabor filters constructed by a genetic algorithm [13] and performed thresholding on the processed image. Zhu *et al.* built a small-scale over-complete basis set via sparse coding to identify defects on patterned fabric [20].

Conventional methods for fabric defect detection proceed in a two-phase fashion: feature extraction and feature identification. The key issue lies in the process of designing distinguishing features. Features could be in the spatial domain, such as LBP, HOG, and covariance matrix, or in the transform domain, such

Manuscript received December 15, 2015; accepted January 15, 2016. Date of publication February 03, 2016; date of current version April 05, 2017. This paper was recommended for publication by Associate Editor Y. Zhang and Editor M. P. Fanti upon evaluation of the reviewers' comments. This research is supported by the Beijing Education Committee Science and Technology Project. *(Corresponding author: Weigang Zhao.)*

Y. D. Li and J. H. Pan are with the School of Electronic and Information Engineering, North China University of Technology, Beijing 100041, China, (e-mail: liyundong@ncut.edu.cn; panjiahao1115@126.com).

W. G. Zhao is with the Institute of Structure Health Monitoring and Control, Shijiazhuang Tiedao University, Shijiazhuang 050043, China (e-mail: zhaoweig2002@163.com).

Color versions of one or more of the figures in this paper are available online at http://ieeexplore.ieee.org.

Digital Object Identifier 10.1109/TASE.2016.2520955

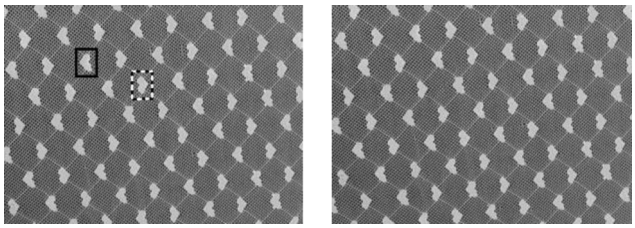

Fig. 1. Examples of patterned warp-knitted fabric.

as Fourier transform, wavelet transform, and Gabor transform. In this study, a completely different solution is explored. Aside from handcrafted features, computers learn fabric features and categorize these features automatically in our scheme.

This research has two main contributions. First, we propose a Fisher criterion-based stacked denoising autoencoders (FCSDA) framework with the objective of improving discrimination for fabric defect detection. As known, SDA has been successfully used in image classification. However, fabric defect detection is slightly different from image classification due to the lack of negative samples. Negative samples, i.e., images with defects, are not conveniently obtained in practice. To overcome the problem, we design a Fisher criterion-based loss function in the feature space, which can improve the detection accuracy when only limited negative samples are available. Second, deep learning is introduced into this field for the first time, and we extend the research subjects from plain, twill and periodic patterned fabric to more complicated jacquard fabric.

The other parts of this paper are structured as follows. Section II presents the target problem and a basic solution. Section III proposes the FCSDA framework. Section IV introduces a novel defect detection scheme based on FCSDA. Sections V and VI focus on the experimental results and discussions. Section VII concludes the research.

II. Problem Formulation

Warp knitting is one of the most prospective knitting methods in textile industry. Warp-knitted fabrics possess soft and deformable attributes and include plain, Jacquard, and other types. In our previous research, we conducted an in-depth study on the defect detection of warp-knitted plain fabric. Approaches with wavelet decomposition and morphology filter were proposed. An embedded machine vision inspection system was developed and operated in a textile factory [21], with a detection brate of 98%.

Although satisfactory results were achieved on plain fabric, defect detection on Jacquard fabric remains challenging in the following aspects. First, the deformable attribute of fabric and lens distortion make nearly all motifs differ slightly in terms of scale and angle. In Fig. 1, two types of motif are marked with solid and dashed rectangles. Second, the texture "moves" in practice, so motifs in the adjacent two frames captured by the image sensor cannot be aligned accurately. Two adjacent frames are shown in Fig. 1; these two cannot be aligned exactly. Third, uneven lighting causes differences in brightness. Given the above points, the ideal defectless image cannot be effectively determined as reference.

Most research efforts focus on plain fabric, and only a few studies tackle jacquard patterned fabric. Zhang *et al.* have studied the segmentation of jacquard warp-knitting fabric with Markov random field [22]. Farooq pointed out that for deformable and complexly patterned fabric, no better means existed than direct comparison with a defectless reference image; in addition, global image processing and regularity-based approaches were unsuitable for this type of fabric [23]. To compare deformable and complexly patterned fabric with a sample fabric, Farooq developed a set of electromechanical devices. A driving motor was installed on a camera, and a synchronous image with patterns was obtained on the sample by adjusting the lens angle. Then, the captured image was directly compared with the reference image.

In this paper, each motif is employed as a patch for detection instead of a whole piece image. Each patch either contains a defect or not. Thus, the defect detection task is converted into an image classification problem. Once a defective patch is marked, the defects are segmented based on the differences between the defective patch and the corresponding reconstruction image.

III. FCSDA Framework

Traditional neural networks consist of an input layer, an output layer, and a single hidden layer, which is called a shallow structure. Neural networks in a shallow structure have limited capability to approximate a complex function. Contrary to the shallow structure, the multiple-hidden-layer structure is called a deep network. Unfortunately, learning in multiple hidden layers has been proven to be difficult in practice. The situation was greatly improved by Hinton in his work published in 2006 [25], [26]. Hinton proposed a greedy layer-wise pretraining algorithm to initialize weights of deep architectures before traditional error BP training. Hinton's work brought renewed vitality to neural networks, and many researchers followed his study and made deep learning a new popular topic. Popular deep learning frameworks include stacked autoencoders, convolutional neural networks, and restricted Boltzmann machine.

A. Sacked Denoising Autoencoders

Let $x \in [0,1]^d$ be the input vector and $y \in [0,1]^d$ be the approximation of x, a traditional autoencoder model is defined as

$$z = f_\theta(x) = s(Wx + b) \tag{1}$$

$$y = g_{\theta'}(z) = s(W'z + b') \tag{2}$$

where $z \in [0,1]^{d'}$ is the hidden representation, W is the weight matrix of $d \times d'$, b is the input bias, $S(\bullet)$ is sigmoid function. An effective representation of input x could be obtained by minimizing a loss function as

$$L(x,y) = \|x - y\|^2. \tag{3}$$

Denoising autoencoder (DA) is an improvement of the traditional autoencoder proposed by Vincent [26] in terms of improving robustness to input noise by corrupting the initial input. A DA is defined as

$$z = f_\theta(\tilde{x}) = s(W\tilde{x} + b) \tag{4}$$

$$y = g_{\theta'}(z) = s(W'z + b'). \tag{5}$$

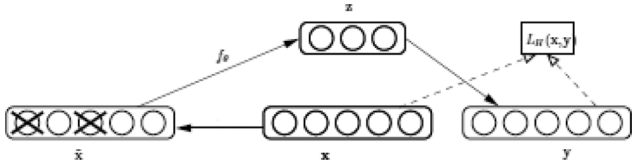

Fig. 2. DA scheme.

The scheme of DA is shown in Fig. 2. In the scheme, $\tilde{x}$ is the corrupted version of the input x. z is activated by $\tilde{x}$ according to (4). y is reconstructed from z according to (5). A loss function same as (3) is utilized to maximize the approximation of the DA output to original noise-free input x. So, z is an effective representation of input x after training.

Stacked DAs are constructed by connecting separately encoding and decoding parts of several DAs in series. The weight matrixes of DAs are employed to initialize the stacked DAs. Suppose we have a fixed training set $\{(x^{(1)}, x^{(1)}), \ldots, (x^{(n)}, x^{(n)})\}$ of n training samples, the entire network is then trained using the standard BP algorithm to minimize the following objective:

$$J_{(W,b)} = \frac{1}{n}\sum_{i=1}^{n}\left(\frac{1}{2}\left\|h_{w,b}(x^{(i)}) - y^{(i)}\right\|^2\right). \tag{6}$$

B. Fisher Criterion-Based SDA

How could we get satisfied detection accuracy in the case that there are only few negative samples when using deep learning in fabric defect detection? It is motivated by the facts that a good feature is expected to preserve the separability between the defective and the defectless patches. Thus, we bring Fisher criterion into the loss function of SDA. Then, loss function in (6) is rewritten as

$$J_{(W,b)} = \frac{1}{n}\sum_{i=1}^{n}\left(\frac{1}{2}\left\|h_{w,b}(x^{(i)}) - y^{(i)}\right\|^2\right) + \lambda\frac{J_{\text{int } ra}}{J_{\text{int } er}} \tag{7}$$

where $J_{\text{int } ra}/J_{\text{int } er}$ is the Fisher criterion in the feature space, λ is a ratio factor. Suppose we have L classes, each class has m_i samples, $i = 1, 2, \ldots, L$. $J_{\text{int}ra}$ and $J_{\text{int}er}$ are the intraclass and interclass distance of features, which are defined as (8) and (9), respectively

$$\begin{aligned} J_{\text{int } ra} &= \frac{1}{2}\sum_{i}^{L}\sum_{k=1}^{m_l}\left\|h_{w,b}(x) - M^{(i)}\right\|^2 \\ &= \frac{1}{2}\sum_{i}^{L}\sum_{k=1}^{m_l}\sum_{j=1}^{s}(a_j^{(k,n_l)} - M_j^{(i)})^2 \end{aligned} \tag{8}$$

$$J_{\text{int } er} = \frac{1}{2}\sum_{i=1}^{L}\sum_{j=i+1}^{L}\left\|M^{(i)} - M^{(j)}\right\|^2 \tag{9}$$

where $h_{w,b}(x)$ is the feature vector abstracted from input x, n_l indicates the output layer of SDA, $a_j^{(k,n_l)} = f(z_j^{(k,n_l)})$ is the $j\text{-}th$ element of the n_l layer feature. $M^{(i)}$ is the average feature of the $i\text{-}th$ class, which is defined as

$$M^{(i)} = \frac{\sum_{k=1}^{m_l} a^{(k,n_l)}}{m_l}, i = 1, 2, \ldots, L. \tag{10}$$

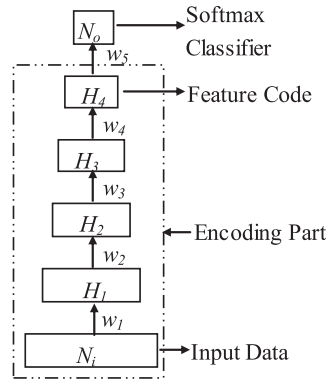

Fig. 3. Structure of FCSDA.

Minimizing the Fisher criterion term of (7) will shorten the intraclass distance, meanwhile, increase the interclass distance. $J_{(W,b)}$ in (7) is minimized by batch gradient descent algorithm in an error BP fashion. Residual error of the output layer is crucial in the calculation procedures. Formula (11) gives the residual error definition of the Fisher criterion term

$$\delta_i^{n_l} = \frac{J_{\text{int } er}\frac{\partial J_{\text{int } ra}}{\partial z_i^{n_l}} - J_{\text{int } ra}\frac{\partial J_{\text{int } er}}{\partial z_i^{(n_l)}}}{{J_{\text{int } er}}^2}. \tag{11}$$

Once $\partial_i^{n_l}$ is calculated, the residual error of other layers are iterated as follows:

$$\delta_i^l = \left(\sum_{j=1}^{s} W_{ji}^{(l)}\delta_j^{l+1}\right) \times \left(a_i^{(l)}(1 - a_i^{(l)})\right). \tag{12}$$

IV. Defect Detection With FCSDA

The proposed FCSDA method for fabric defect detection has two steps: FCSDA training and defect detecting.

A. FCSDA Training

The proposed FCSDA consists of four hidden layer and a softmax classifier, shown as Fig. 3. Only the encoding part is displayed in Fig. 3. The training proceeds in a two-phase fashion: pretraining and fine-tuning. First, training set is constructed with patches drawn from images captured by industry cameras. The training set includes both positive samples and negative samples. Second, each DA is trained in an unsupervised manner. Third, weight and bias parameters of DAs are used to initialize FCSDA instead of random values. Fourth, FCSDA is fine-tuned by supervised learning with labeled dataset. There are total $(N_i + 1)^*H_1 + (H_1 + 1)^*H_2 + (H_2 + 1)^*H_3 + (H_3 + 1)^*H_4 + (H_4 + 1)^*N_o$ weights and biases should be trained in the Fig. 3 architecture. We can visualize the weights to demonstrate what features are learnt by FCSDA. Samples such as those in Fig. 4 are exploited to train the FCSDA in this test. Fig. 5 shows some weights of the first DA as little image patches. Each patch corresponds to a row of the weight matrix. We can clearly see that the DA has learned some interesting features which appear to be abstracts of the input patterns. Studies have shown that the feature abstract procedure is conformed to the learning process of human brain.

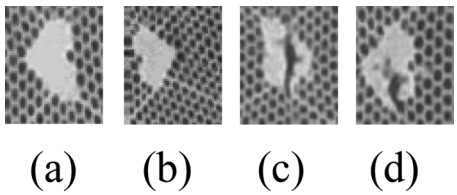

Fig. 4. Three types of patterns. (a) Pattern 1. (b) Pattern 2. (c) Defective pattern. (d) Defective pattern.

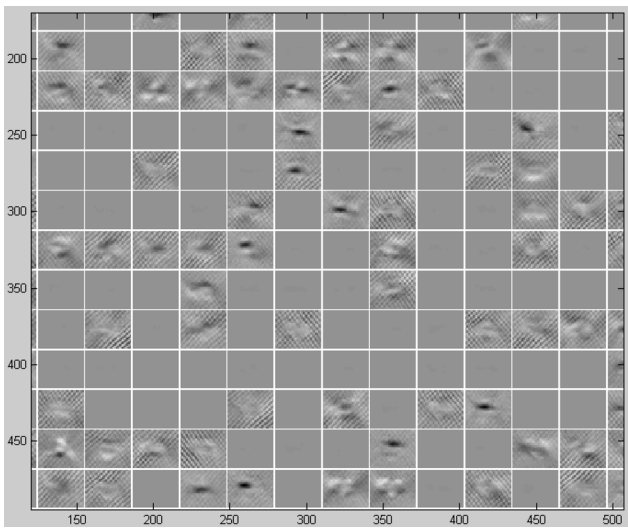

Fig. 5. Visualization of weights.

B. Fisher Criterion Optimization

Fisher criterion optimization proceeds on the last hidden layer in the fine-tuning phase. Outputs of the last hidden layer are utilized to calculate residual error according to formula (11). Then, all the weights and biases are adjusted according to residual error. Optimization of Fisher criterion can guide the learning direction of deep networks, which makes the feature distribution has a clear physical meaning. We can prove this by experimental results comparison shown in Fig. 6. We plot the Fisher criterion term of FCSDA and the traditional SDA after each training epoch, respectively. It is clearly shown that $J_{\text{int } ra}/J_{\text{int } er}$ of FCSDA is smaller than that of the traditional SDA. This means features abstracted by FCSDA have better discrimination than that of SDA.

C. Defect Detecting

FCSDA is ready for defect detection after training. The flowchart is shown in Fig. 7. There are two FCSDAs in Fig. 7, where FCSDA1 is used to classify test patches into defectless or defective categories, and FCSDA2 is used to reconstruct the input patches.

1) Image Reconstruction: Once the defective patches are marked, the defects could be located through the differences between the defective patches and the reconstructed images. The reconstructed image is crucial to the locating accuracy. In practice, we found that the reconstructed images obtained from FCSDA1 in Fig. 7 are well matched with the input patches. So, the differences don't have any useful information about defects

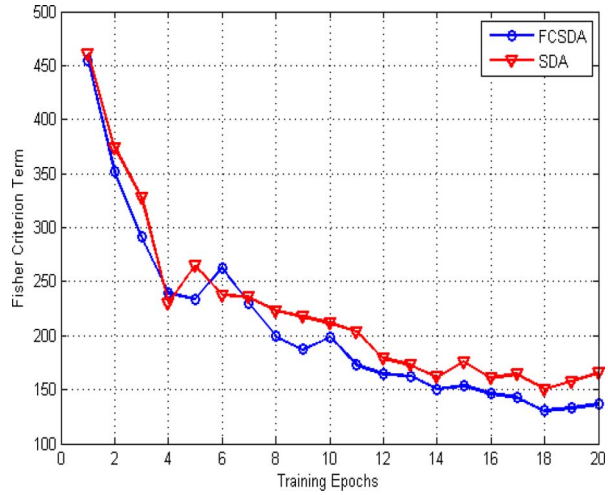

Fig. 6. Fisher criterion term comparison between FCSDA and SDA.

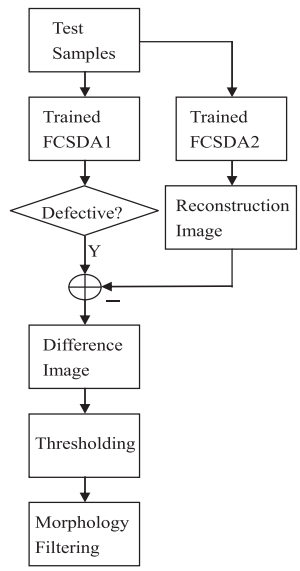

Fig. 7. Flowchart of defect detection and locating.

because the reconstructed images are very similar to the original defective images. An ideal reconstructed image is expected to have no defect area, meanwhile, remaining similar outline with the defective patch. We proposed a novel method to reconstruct the defective patches through another FCSDA2, which has the similar architecture and parameters with FCSDA1. Fig. 3 shows the structure of FCSDA1 and the structure of FCSDA2 is shown in Fig. 8. It is worth noting that softmax classifier is no longer needed in FCSDA2, as well as the supervised fine-tuning and the Fisher criterion optimization. Another difference between FCSDA1 and FCSDA2 is the training set. Both defectless and defective samples are utilized to train FCSDA1, however, only the defectless samples are exploited to train FCSDA2.

The reconstruction process is described as follows: First, the defective patch is inputted into the encoding part of FCSDA2 to obtain the feature code. Second, the feature code is inputted into the decoding part of FCSDA2 according to formula (5). Finally, the reconstruction image is obtained from the output of FSCDA2. Part of the reconstruction images are shown in

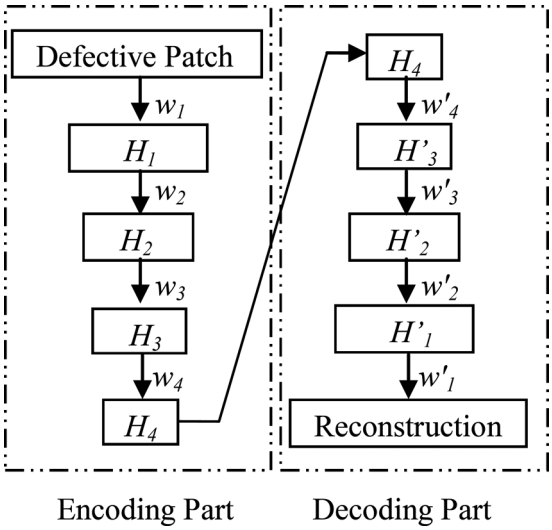

Fig. 8. Structure of FCSDA2 and the data reconstruction process.

Fig. 11. The experimental results demonstrate that our reconstruction method is very effective.

2) Locating the Defects: The testing set, including defectless and defective samples, are inputted into FCSDA1 in Fig. 7. A softmax classifier is utilized to identify the sample as defectless pattern or defective pattern. When the testing sample is identified as a defective pattern, the difference image between this sample and the reconstructed image is calculated. Then, the defect can be located by thresholding and morphology filtering this binary image.

V. Experimental Results

To evaluate the performance of the proposed FCSDA method, we compared it with ID method [18] and the traditional SDA method for periodic pattern and jacquard pattern fabrics, respectively. The testing code was implemented under MATLAB version R2012B. The testing computer was configured with Intel i5 processor with 3.2 GHz frequency and 8.0 GB memories. A group of metrics including accuracy (ACC), true positive rate (TPR), false positive rate (FPR), and positive predictive value (FPV), were employed to quantify the locating accuracy [18]. The definition of ACC, TPR, FPR, and FPV are described as formula (13)–(16)

$$ACC = \frac{(TP + TN)}{(TP + TN + FP + FN)} \tag{13}$$

$$TPR = \frac{TP}{(TP + FN)} \tag{14}$$

$$FPR = \frac{FP}{(FP + TN)} \tag{15}$$

$$PPV = \frac{TP}{(TP + FP)} \tag{16}$$

where true positive (TP), true negative (TN), false positive (FP), and false negative (FN) are labeled in Fig. 9.

A. Experiment 1—Defect Detecting for Periodic Pattern

In the literature, the ID method obtained the best reported results on the benchmark fabric images with periodic pattern

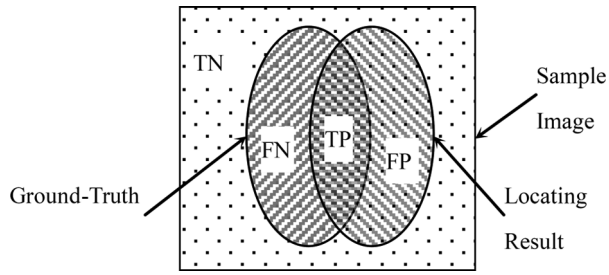

Fig. 9. Definitions of TN, FN, TP, and FP.

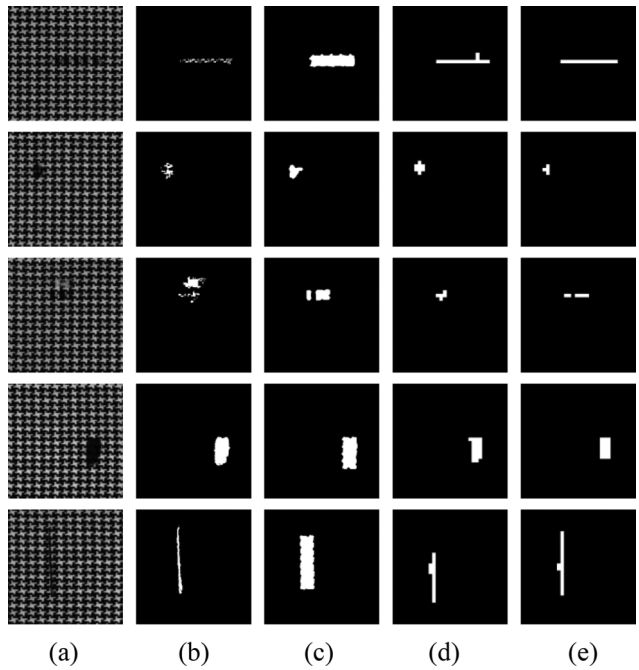

Fig. 10. Defect locating results comparison. (a) Defective images. (b) The ground-truths labeled by manual. (c) Results of ID method. (d) Results of SDA method. (e) Results of FCSDA method.

[18], [19]. In this experiment, we used FCSDA to detect defects on the same images. The patches with 8×8 sizes were drawn from these images. In this experiment, the numbers of hidden layer were set to 3, which was slightly different from Fig. 3. The numbers of neurons in each layer were 64, 600, 200, 100, and 2, respectively. In this experiment, learning rate of FCSDA was set to 0.8, scaling factor was 0.9, $\lambda = 0.12$.

Five star-patterned fabric images were used as benchmark, and the defect locating results are shown in Fig. 10. All the defects were detected by ID, SDA and FCSDA methods. The locating accuracies are listed in Table I, and the best results are marked in bold. FCSDA gets 13 of the highest scores in 20 testing items. Though ID method achieves high scores on TPR, FCSDA performs well than ID method on ACC, FPR, and PPV metrics. Especially, FCSDA achieves highest ACC scores on "BrokenEnd," "Hole," "NettingMultiple," and "ThinBar" defects. ACC is the most important metric which can quantify the locating accuracy comprehensively. Basing the analyses above, we state that FCSDA method is superior to the ID and SDA methods in locating accuracy. Herein, we would like to express our gratitude to Dr. H. Y. T. Ngan who provided benchmark images and test codes.

TABLE I
LOCATING ACCURACY COMPARISON OF EXPERIMENT 1

Defect Types	Methods	ACC (%)	TPR (%)	FPR (%)	PPV (%)
Broken End	ID	96.50	**81.99**	3.42	11.73
	SDA	98.58	73.96	1.28	24.18
	FCSDA	**98.66**	70.08	**1.18**	**24.71**
Hole	ID	99.14	**50.89**	0.61	**30.16**
	SDA	99.02	30.65	0.63	20.12
	FCSDA	**99.21**	10.71	**0.34**	14.06
Netting Multiple	ID	97.76	**19.31**	1.22	17.14
	SDA	98.42	8.41	0.41	21.13
	FCSDA	**98.50**	14.34	**0.41**	**31.51**
Thick Bar	ID	**99.19**	**97.99**	0.77	78.07
	SDA	99.06	70.23	0.13	93.94
	FCSDA	98.95	63.07	**0.04**	**97.83**
Thin Bar	ID	95.20	**83.29**	4.66	17.35
	SDA	97.89	30.79	1.32	21.51
	FCSDA	**98.21**	57.11	**1.31**	**33.91**

B. Experiment 2—Defect Detecting for Jacquard Pattern

As mentioned before, defect inspection for jacquard pattern fabric is more challenging. In this experiment, fabrics such as Figs. 1 and 4 were used as test benchmark. The architecture shown in Fig. 3 was employed in this experiment. The patches with 30×25 sizes were drawn from images captured by industry cameras. Each patch was converted into a 750-dimension vector as the input of FCSDA. The numbers of neurons in each layer were 750, 600, 400, 200, 100, and 3, respectively. In this experiment, learning rate of FCSDA was set to 0.5, scaling factor was 0.9, $\lambda = 0.12$.

We gathered 2600 patches as samples, among which are 2000 pieces of positive samples, and 600 pieces of negative samples. The motifs in these patches differ in scale, angle, and brightness. The position of each motif in the patches differs as well. All 2600 samples were divided into two sets: 2000 in the training set and 600 in the testing set (which contains 400 defectless and 200 defective samples).

To evaluate the performance of FCSDA, the ID method, and the SDA method were used for comparisons. We found that ID method cannot separate out the defects from the original images. So, the patches were reversed to enhance the defect areas first, and then decomposed by ID method. The reversion process is described as formula (17)

$$I_{ij} = 255 - I_{ij} \tag{17}$$

where I_{ij} is the pixel value.

Testing set with 600 samples is inputted into trained deep networks, the detection results of SDA and FCSDA are shown in Table II, as well as the detection results of ID method.

TABLE II
DETECTION RATIO COMPARISON OF EXPERIMENT 2

Methods	FA (%)	DR (%)	ODR (%)
ID	7.75	85.00	89.83
SDA	3.75	91.00	94.50
FCSDA	**2.50**	**92.50**	**95.83**

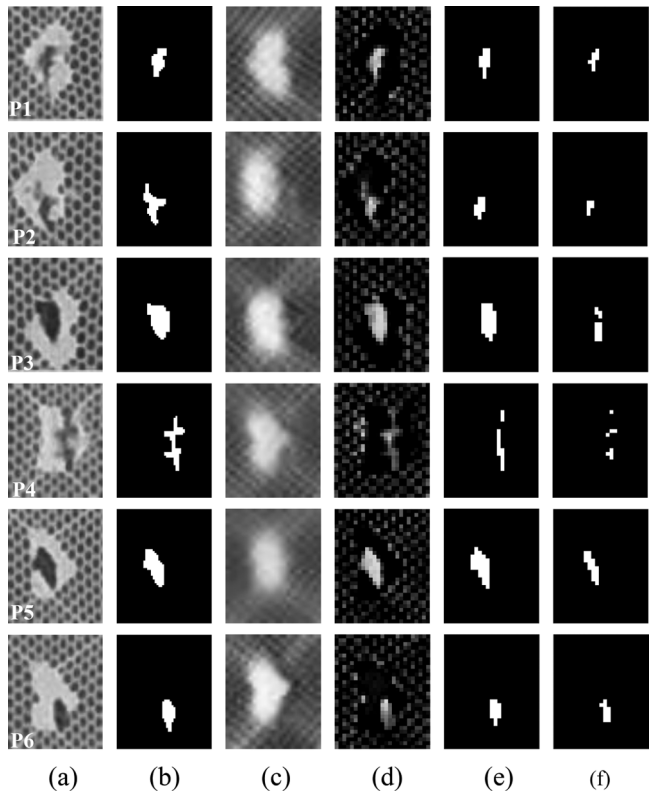

Fig. 11. Locating results of three testing methods. (a) Original patches. (b) Ground-truths. (c) Reconstructed images. (d) Difference images. (e) Final results of FCSDA and SDA methods. (f) Final results of ID method.

Besides ACC, TPR, FPR, and FPV used in the last experiment, another group metrics including false alarm (FA), detection rate (DR), and overall detection rate (ODR), were selected to evaluate the detection ratios. FA is the ratio of defectless samples falsely identified as defective samples. DR is the ratio of correctly identified defective samples. ODR is the ratio of all correctly identified samples. FA and DR cannot be employed separately, and our focus is to increase DR in the premise of maintaining low FA. Table II clearly indicates that the performance of FCSDA method is significantly better than ID method. Further, FCSDA method is also superior to the traditional SDA method on FA, DR, and ODR metrics.

The defects in a patch can be located after detection with FCSDA1. If a patch is identified as a defective one, then first, the difference image between reconstruction and this defective patch is obtained. Second, thresholding is applied to the difference image, and a binary image is produced. Finally, the defect location is obtained after morphology filtering. The defect segmentation results by three testing methods are shown in Fig. 11. We select the detection results of six defective patches (P1–P6), which represent three types of defects,

TABLE III
LOCATING ACCURACY COMPARISON OF EXPERIMENT 2

Defect Types	Methods	ACC (%)	TPR (%)	FPR (%)	PPV (%)
	ID	98.80	50.00	**0**	**100**
P1	SDA	**99.20**	**77.78**	0.27	87.50
	FCSDA	**99.20**	**77.78**	0.27	87.50
	ID	97.96	21.43	**0**	**100**
P2	SDA	**98.00**	**46.43**	**0**	**100**
	FCSDA	**98.00**	**46.43**	**0**	**100**
	ID	96.27	31.58	**0.28**	85.71
P3	SDA	**98.27**	**76.32**	0.56	**87.88**
	FCSDA	**98.27**	**76.32**	0.56	**87.88**
	ID	96.27	20.59	**0.14**	**87.50**
P4	SDA	**97.07**	**41.18**	0.28	**87.50**
	FCSDA	**97.07**	**41.18**	0.28	**87.50**
	ID	98.67	65.52	**0**	**100**
P5	SDA	**99.47**	**100**	0.55	87.88
	FCSDA	**99.47**	**100**	0.55	87.88
	ID	98.80	55.00	**0**	**100**
P6	SDA	**99.20**	**80.00**	0.27	88.89
	FCSDA	**99.20**	**80.00**	0.27	88.89

namely, hole, dot, and thin bar. Fig. 11(a) illustrates the original patches, Fig. 11(b) shows the manual-labeled ground-truths, Fig. 11(c) indicates the reconstruction images, Fig. 11(d) is the differences between defective patches and reconstructions, Fig. 11(e) illustrates the defects located by FCSDA and SDA methods, and Fig. 11(f) gives the defects located by ID method.

Fig. 11 shows that the defect segmentations by FCSDA and SDA methods are more accurate than the ID method.

Further, we use ACC, TPR, FPR, and FPV metrics to quantify the locating accuracies of the three testing methods. The accuracy comparison is listed as Table III, and the best results are marked in bold. We can see that FCSDA and SDA methods are significantly better than ID method on ACC and TPR metrics, and get 16 of highest scores in 24 testing items. Generally speaking, the FCSDA and SDA methods are superior to the ID method on detection ratio and locating accuracy.

As mentioned before, Fisher criterion optimization is not needed in the reconstruction process. So, the FCSDA and SDA methods share the same reconstruction images and have the same locating accuracy.

VI. DISCUSSION

A. Relationship Between DA Number and Results

FCSDA is composed of several DAs, and in this section, we discuss the relationship between DA number and detection results. Table IV lists the detection results when the DA number varies from 2 to 5. The best result is clearly achieved with four

TABLE IV
RELATIONSHIP BETWEEN DA NUMBER AND RESULTS

Number of DA	FA (%)	DR (%)	ODR (%)
2	2.75	89.0	94.0
3	3.25	90.0	94.0
4	2.50	92.5	95.8
5	3.00	83.0	92.3

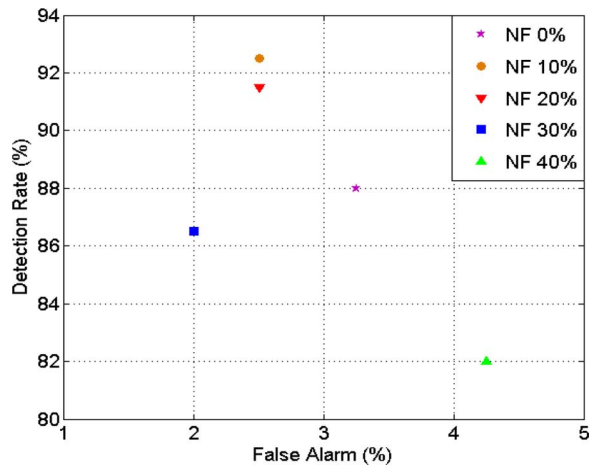

Fig. 12. FA and DR values with various NF.

DAs. The performance of FCSDA with two and three DAs are slightly worse than that of four DAs. When the DA number is too small, deep learning cannot learn effective representations. Therefore, the detection results in this situation are worse than those with four DAs. Theoretically, five DAs should outperform four DAs. However, a five-DA deep network has more parameters to be trained than those of four-DA architecture. More samples are needed to train the five-DA deep network. So, its performance will deteriorate with insufficient training and is not as good as that of four DAs.

B. Comparison of the Effect of Various Noise Fractions

The jacquard fabric is soft and easily deformable. Each patch may be different in brightness, scale, and rotation angles. Noises are added into input data during training in terms of improving the robustness. Many implementations for DA exist, and the simplest method is to set randomly partial input component to zero in a certain proportion, which is called the noising fraction (NF). Here, we attempt to evaluate the effect of NF on detection accuracy. Fig. 12 shows detection FA and DR with different NF values. NF $= 10\%$ provides the best result. Fig. 13 shows ODR values with different NF, and maximum ODR appears when NF $= 10\%$. The experimental results in Figs. 12 and 13 indicate that proper NF can improve performance. We can obtain a conclusion that DA performance appears to be a parabolic curve respect to NF. There is trivial meaning when NF is too small. However, performance will decrease significantly if NF is too large. This can be understood from the manifold learning perspective [26]. Suppose positive samples concentrate near a low-dimensional manifold. Naturally, negative samples lie far from the manifold. The positive samples corrupted by larger NF

Fig. 13. ODR values with various NF.

cannot be projected back to the manifold by DA and will be incorrectly identified as defective ones.

C. Timing Spent Analysis

The training process of FCSDA is time-consuming. In the second experiment, the training time can reach 296.9 s. However, the FCSDA method can still be employed for real-time inspection because the training phase is implemented offline. The online detection process is very quickly. In our experiment, average detection time of each patch is 0.21 ms, which can meet the real-time inspection demands.

D. Hyper-Parameters Selection

The parameters of deep networks, such as learning rate, network depth, number of hidden layer units, are called "hyper-parameters," which require practical experiences to decide how to set the values [27]. The brute-force search according to the final detection accuracy is not recommended. Herein, we discuss the practiced principles that have been successfully used in tuning deep multilayer networks.

- **Learning rate** α. Learning rate is very crucial to gradient-based learning algorithms. Network weights are updated according to formula (18) after each training batch. A much large value of α will cause the training divergence, however, a small value will slow the training process. A heuristic principle is choosing a value close to the largest learning rate that does not cause divergence [28]. In practice, we start with a large value within (0,1), and if the loss increases, decrease the value, until no divergence is observed

$$W_{ij}^{(k)} = W_{ij}^{(k-1)} + \alpha \frac{\partial J_{(W,b)}}{\partial W_{ij}^{(k-1)}}. \tag{18}$$

- **Scaling factor** β. Learning rate can be kept constant during the training process. However, a decay of learning rate sounds more reasonable along with the training process, which benefits from avoiding missing the optimal gradient-descent direction. In our experiments, learning rate is updated by $\alpha = \beta\alpha$ after each epoch, and β is set to 0.9.
- **Network depth and number of hidden layer units**. The network depth, i.e., number of DAs, has been discussed in Section VI-A. As for the number of hidden layer units, a basic principle is an over-complete first hidden layer will work better [28], i.e., the number of first hidden units are larger than that of the input layer. In experiment 1, the input layer units are 64, and the first hidden units are 600, which is large than that of input layer. In experiment 2, the number of first hidden units is chosen close to 750 (the number of input units) because a larger number will lead to more computation.

VII. Conclusion

In this paper, we propose a Fisher criterion-based SDA framework with the objective of learning more discriminative features, which can efficiently inspect defects for both periodic pattern and jacquard pattern fabrics. Benefiting from optimization of Fisher criterion in feature space, we can obtain satisfied detection accuracy even the negative samples are insufficient. The proposed method provides solutions to defect inspection for complex patterned textile that have not been tackled before. We extend the research subjects from plain, twill and periodic patterned fabric to more complicated jacquard fabric. In addition, FCSDA-learnt features have good adaptability to the brightness variation and deformation, such as scale and rotation angle variant. In the future, we would like to explore how to integrate this method into an automatic defect inspection system.

Acknowledgment

This research is supported by the Beijing Education Committee Science and Technology Project.

References

[1] H. Y. T. Ngan, G. K. H. Pang, and N. H. C. Yung, "Automated fabric defect detection-A review," *Image Vision Comput.*, vol. 29, no. 7, pp. 442–458, 2011.
[2] D. Schneider and D. Merh, "Blind weave detection for woven fabrics," *Pattern Anal. Appl.*, vol. 18, no. 3, pp. 725–737, 2015.
[3] G. Hu, Q. Zhang, and G. Zhang, "Unsupervised defect detection in textiles based on Fourier analysis and wavelet shrinkage," *Appl. Opt.*, vol. 54, no. 10, pp. 2963–2980, 2015.
[4] E. Mohamed, H. Mounir, Q. Khadijah, and S. Ebraheem, "Application of principal component analysis to boost the performance of an automated fabric fault detector and classifier," *Fibres Textiles in Eastern Europe*, vol. 22, no. 4, pp. 51–57, 2014.
[5] M. As, J. Y. Drean, L. Bigue, and J. F. Osselin, "Optimization of automated online fabric inspection by fast Fourier transform (FFT) and cross-correlation," *Textile Res. J.*, vol. 83, no. 3, pp. 256–268, 2013.
[6] B. Zhu, J. Liu, R. Pan, W. Gao, and J. L. Liu, "Seam detection of inhomogeneously textured fabrics based on wavelet transform," *Textile Res. J.*, vol. 85, no. 13, pp. 1381–1393, 2015.
[7] P. F. Li, H. H. Zhang, J. F. Jing, R. Z. Li, and J. Zhao, "Fabric defect detection based on multi-scale wavelet transform and Gaussian mixture model method," *J. Textile Inst.*, vol. 106, no. 6, pp. 587–592, 2015.
[8] G. H. Hu, G. H. Zhang, and Q. H. Wang, "Automated defect detection in textured materials using wavelet-domain hidden Markov models," *Opt. Eng.*, vol. 53, no. 9, 2014.
[9] Z. J. Wen, J. J. Cao, X. P. Liu, and S. H. Ying, "Fabric defects detection using adaptive wavelets," *Int. J. Clothing Sci. Technol.*, vol. 26, no. 3, pp. 202–211, 2014.
[10] C. H. Ibrahim, T. Mehmet, and D. L. Canan, "Real-time denim fabric inspection using image analysis," *Fibres Textiles in Eastern Europe*, vol. 23, no. 3, pp. 85–90, 2015.
[11] G. H. Hu, "Automated defect detection in textured surfaces using optimal elliptical Gabor filters," *Optik*, vol. 126, no. 14, pp. 1331–1340, 2015.
[12] L. Bissi, G. Baruffa, P. Placidi, E. Ricci, A. Scorzoni, and P. Valigi, "Automated defect detection in uniform and structured fabrics using Gabor filters and PCA," *J. Vis. Commun. Image R*, 2013.

[13] J. F. Jing, P. P. Yang, P. F. Li, and X. J. Kang, "Supervised defect detection on textile fabrics via optimal Gabor filter," *J. Ind. Textiles*, vol. 44, pp. 40–57, 2014.
[14] H. I. Celik, L. C. Dulger, and M. Topalbekiroglu, "Fabric defect detection using linear filtering and morphological operations," *Indian J. Fibre Textile Res.*, vol. 39, no. 3, pp. 254–259, 2014.
[15] H. I. Çelik, L. C. Dülger, and M. Topalbekiroglu, "Development of a machine vision system: Real-time fabric defect detection and classification with neural networks," *J. Textile Inst.*, vol. 105, no. 6, pp. 575–585, 2014.
[16] Y. M. Song, D. L. Yuan, Y. F. Lu, and G. H. Qiao, "Automated detection of fabric defects based on optimum PCNN model," *Chinese J. Scientific Instrum.*, vol. 29, no. 4, pp. 888–891, 2008.
[17] S. W. Zhu and C. H. Hao, "An approach for fabric defect image segmentation based on the improved conventional PCNN model," *Acta Electronica Sinica*, vol. 40, no. 3, pp. 611–616, 2012.
[18] M. K. Ng, H. Y. T. Ngan, X. M. Yuan, and W. X. Zhang, "Patterned fabric inspection and visualization by the method of image decomposition," *IEEE Trans. Autom. Sci. Eng.*, vol. 11, no. 3, pp. 943–947, Oct. 2014.
[19] M. K. Ng, X. M. Yuan, and W. X. Zhang, "A coupled variational image decomposition and restoration model for blurred cartoon-plus-texture images with missing pixels," *IEEE Trans. Image Process.*, vol. 22, pp. 2233–2246, Jun. 2013.
[20] Q. P. Zhu, M. Y. Wu, J. Li, and D. X. Deng, "Fabric defect detection via small scale over-complete basis set," *Textile Res. J.*, vol. 84, no. 15, pp. 1634–1649, 2014.
[21] Y. D. Li, J. X. Ai, and C. Q. Sun, "Fabric defect inspection using smart visual sensors," *Sensors*, vol. 13, no. 4, pp. 4659–4673, 2013.
[22] Y. Zhang, G. Jiang, J. Yao, and Y. Tong, "Intelligent segmentation of jacquard warp-knitted fabric using a multiresolution Markov random field with adaptive weighting in the wavelet domain," *Textile Res. J.*, vol. 84, no. 1, pp. 28–39, 2014.
[23] U. Farooq, T. King, P. H. Gaskell, and N. Kapur, "Machine vision using image data feedback for fault detection in complex deformable webs," *Trans. Inst. Meas. Control*, vol. 26, no. 2, pp. 119–137, 2004.
[24] G. E. Hinton and R. R. Salakhutdinov, "Reducing the dimensionality of data with neural networks," *Sci.*, vol. 313, no. 5786, pp. 504–507, 2006.
[25] G. E. Hinton, S. Osindero, and Y. W. Teh, "A fast learning algorithm for deep belief nets," *Neural Comput.*, vol. 18, no. 7, pp. 1527–1554, 2006.
[26] P. Vincent *et al.*, "Extracting and composing robust features with denoising autoencoders," in *Proc. 25th Int. Conf. Mach. Learn.*, New York, NY, USA, 2008, pp. 1096–1103.
[27] G. Hinton, "A practical guide to training restricted Boltzmann machines," *Lecture Notes in Comput. Sci.*, vol. 7700, pp. 599–619, 2012.
[28] Y. Bengio, "Practical recommendations for gradient-based training of deep architectures," *Lecture Notes in Comput. Sci.*, vol. 7700, pp. 437–478, 2012.

Yundong Li received the Ph.D. degree from the Beihang University, Beijing, China, in 2005.

He is currently a Lecturer with the Faculty of Electronic and Information Engineering, North China University of Technology, Beijing, China. His research interests include machine learning, neural networks, computer vision and fabric defect inspection.

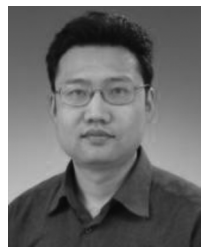

Weigang Zhao received the Ph.D. degree from the Beihang University, Beijing, China, in 2009.

He is currently a Professor with the Institute of Structure Health Monitoring and Control, Shijiazhuang Tiedao University, Shijiazhuang, China. His research focus is intelligent information processing, spread spectrum communication and structural health monitoring.

Jiahao Pan received the B.S. degree from the Changshu Institute of Technology at Changshu, Changshu, China, in 2013. He is currently working towards the M.S. degree in electronic science and technology at North China University of Technology, Beijing, China.

His research focus is computer vision and image processing.